12th Symposium on Measuring Techniques
for Transonic and Supersonic Flow in Cascades and Turbomachines

Prague, Czech Republic, September 12-13,1994

DYNAMIC RESPONSE OF AERODYNAMIC PROBES IN FLUCTUATING 3D FLOWS

H.J. Humm, W. Gizzi, G. Gyarmathy
ETH Zurich
Switzerland

Dynamic Response of Aerodynamic Probes in Fluctuating 3D Flows

H.J. Humm, W.P. Gizzi, G. Gyarmathy

Institute of Energy Technology
Turbomachinery Laboratory
Swiss Federal Institute of Technology, Zurich

The influence of pitch angle and velocity fluctuations on the characteristics of aerodynamic probes was investigated experimentally. In context with earlier experiments reported in HUMM/ VERDEGAAL (1992A), where dynamic effects due to yaw angle fluctuations were investigated, the dynamic response of probes to fully 3D flow fluctuations can now be quantified.

In the model-experiments enlarged probes forced to oscillate were towed in a water channel. In this dynamic flow environment, simulating conditions inside turbomachines, the time dependent response of the probes was recorded. The comparison of the dynamic characteristics to the quasi static reference values shows enormous deviations. This implies that inevitable measurement errors may occur when static calibration characteristics are applied without prejudice for the evaluation of dynamic signals.

Some of the dynamic effects which would lead to severe measurement errors can be completely avoided whereas other effects remain. From the latter, within limits, an important group shows a systematic behaviour. For these a mathematical model describing the effects is presented. The knowledge of the relations between flow fluctuation and response of the probes can later be used for correcting measurement errors due to dynamic effects.

1. INTRODUCTION

When applying aerodynamic probes for fast-response measurements in turbomachines a great number of aerodynamic effects have to be carefully considered in order to avoid measurement errors and to achieve a good accuracy.

At the Laboratory, the influence of Reynolds and Mach number, velocity gradients, vortex interaction, blockage, turbulence effects and flow angle on the pressure indicated by probes was investigated experimentally and theoretically.

Probes used for measurements in turbomachines are exposed to strong dynamic flow conditions. The main question arising in this context is to what extent the aerodynamic characteristics of fast-response probes (usually obtained from static calibration e.g. in a wind tunnel) are changed in a dynamic environment.

Investigations concerning dynamic aerodynamic effects have been gaining in importance in many engineering areas. Especially in offshore technology, flutter prediction and prevention in aircraft and missile development, buildings, bridges and underwater cable systems dynamic aerodynamic effects have become a fundamental research topic (McCROSKEY 1977, NAUDASCHER 1991). E.g. designers of helicopters have for long taken advantage of the fact

that under dynamic conditions the airload on rotors can be remarkably increased. If subjected to dynamic flows, where incidence angles are time dependent, dynamic stall on the airfoils leads to enormous pressure drops on the suction side, improving the lift of the rotors by a great amount.

First investigations concerning the response of aerodynamic probes in fluctuating flows were performed by KOVASZNAY et al. (1981). Spherical probes were exposed to a pulsating air jet and the pressure as a function of the time dependent velocity was recorded. The objective of the present work is to determine the dynamic aerodynamic characteristics of probes in time variant 3D flows. This includes

- experiments with controlled flow angle fluctuations (yaw and pitch) in addition to velocity fluctuations

- comparison of the dynamic characteristics of various probe shapes

Apart from dynamic effects due to external flow fluctuation an additional dynamic effect is caused by vortex-interaction. The Kármán vortex shedding imposes a fluctuating potential field on the flow around probes.

In turbomachines the magnitude of free stream velocities ranges typically from $c_\infty = 100$ to 450 m/s and the blade passing frequencies from $f = 2$ kHz to 10 kHz. For measurements usually probes of $2 < D < 5$ mm tip width are applied. Thus the Reynolds number is of the order of $Re_D = 10'000$ to 120'000. The Mach number is typically in the range from 0.3 to 1.3. The governing parameter for dynamic processes, the reduced frequency $k = f D / c_\infty$, lies between 0.05 and 0.5. The creation of such a flow environment with reference quality, where the dynamic response of probes can be determined experimentally, lies far beyond technical feasibilities. Thus for the investigations performed at the Laboratory the strategy of model-experiments in water was adopted (HUMM/VERDGAAL 1992A).

In chapter 2 of this paper the experimental facilities are briefly described. The results of the experiments are presented in chapter 3. In the sections 3.1 to 3.3 the parameters influencing the dynamic behaviour of probes exposed to dynamic flows are discussed and in section 3.4 the suitability of probes for measurements in turbomachines. The mathematical modelling and compensation of dynamic effects is described in chapter 4 leading to the conclusions in chapter 5.

2. EXPERIMENTAL FACILITIES

Model-experiments were performed in a water channel with a total length of 40 m and a cross section of 1 m². The experimental set-up is described in detail in HUMM/VERDGAAL (1992A). Scaled-up probes with a diameter of 30 mm were towed in stationary water while a controlled oscillatory motion was imposed.

With the aid of these experiments a dynamic environment representing the conditions in turbomachines was simulated with very low frequencies of oscillations ($1 < f < 10$ Hz) and low free stream velocities ($0.7 < c_\infty < 2.8$ m/s). The Reynolds number was kept at realistic values (i.e. varied between 20'000 and 160'000) whereas the influence of the Mach number had to be neglected.

Figure 2-1 shows the oscillating mechanism for the model-experiments. During the experiments the reduced frequency was varied from $k = 0.05$ to 0.4 by changing the frequency of the DC-

motor. The amplitudes of the angular motion could be varied in a range from 0° to ± 45°. In terms of $\hat{\alpha}$ this represents typical conditions in turbomachines where the systematic periodic mean yaw angle covers a range of approximately $\pm\,\bar{\alpha} \approx 20°$. Depending on the turbulence level, transient flow angles may stochastically exceed this range by as much as approximately additional ± 10° (GOSSWEILER et al. 1992). In terms of pitch smaller amplitudes $\hat{\gamma}$ would suffice, too (see section 3.4).
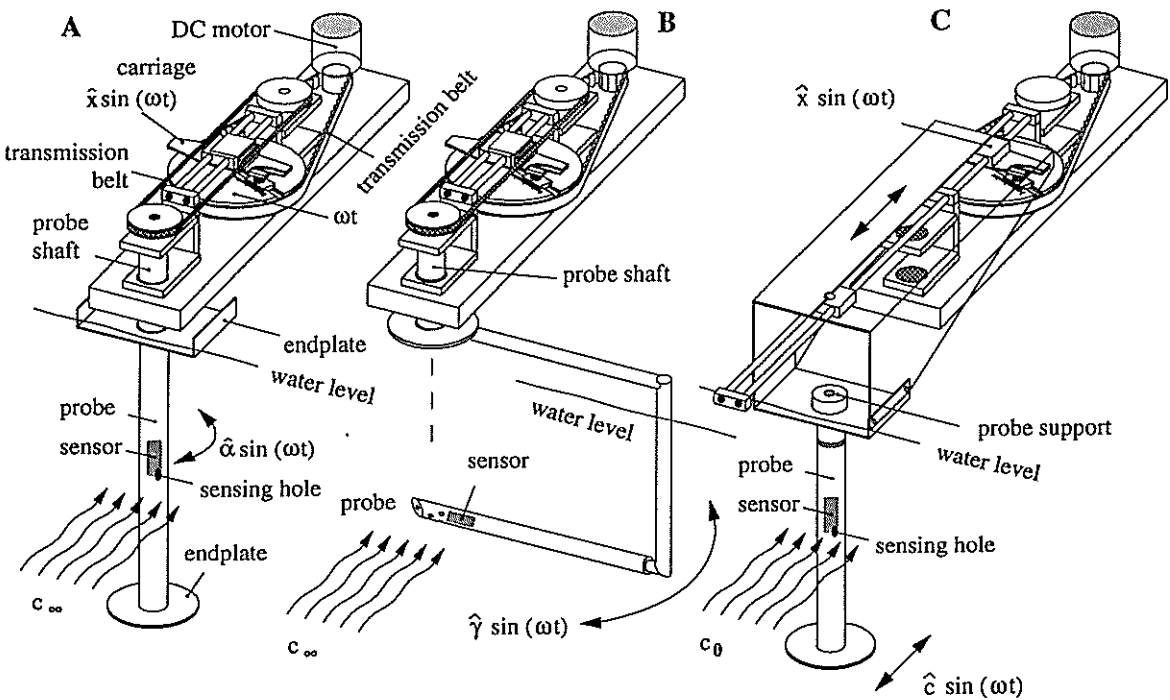

Figure 2-1   Oscillating mechanism for dynamic calibration; yaw angle (A), pitch angle oscillations (B) and velocity oscillations (C)

It had to be ensured that the forced motion of the probes did not affect the accuracy of pressure measurement. In the case of pitch angle oscillations preceding the experiments the effect of acceleration forces acting on the sensor - which could not be placed in the rotation center - and on the water enclosed in the probe interior had to be determined.

During the experiments the time dependent pressures indicated by the sensor inside the probe were recorded. The pressures were ensemble averaged with respect to a simultaneously registered trigger signal over several periods of oscillation. These phase locked averages were then plotted versus the forced angle (yaw and pitch) or velocity, respectively and quantitatively compared to the static reference characteristic.

3. RESULTS

3.1 YAW ANGLE OSCILLATIONS

In addition to the results presented in HUMM/VERDEGAAL (1992A), where the influence of yaw angle oscillations were systematically investigated, the characteristics of a 3-D cone probe and a half cylinder were determined. The reason for the dynamic calibration of the latter was to investigate whether Kármán vortex-interactions (see discussion below) could be reduced by applying trailing edges on a bluff probe body. In figure 3.1-1 the dynamic pressure coefficients c_{p_1} (α) of all probes tested are plotted versus the forced flow angle α (t) and compared to the static characteristics. The data shown refer to a constant reduced frequency k = 0.1 and to different amplitudes of oscillation $\hat{\alpha}$.
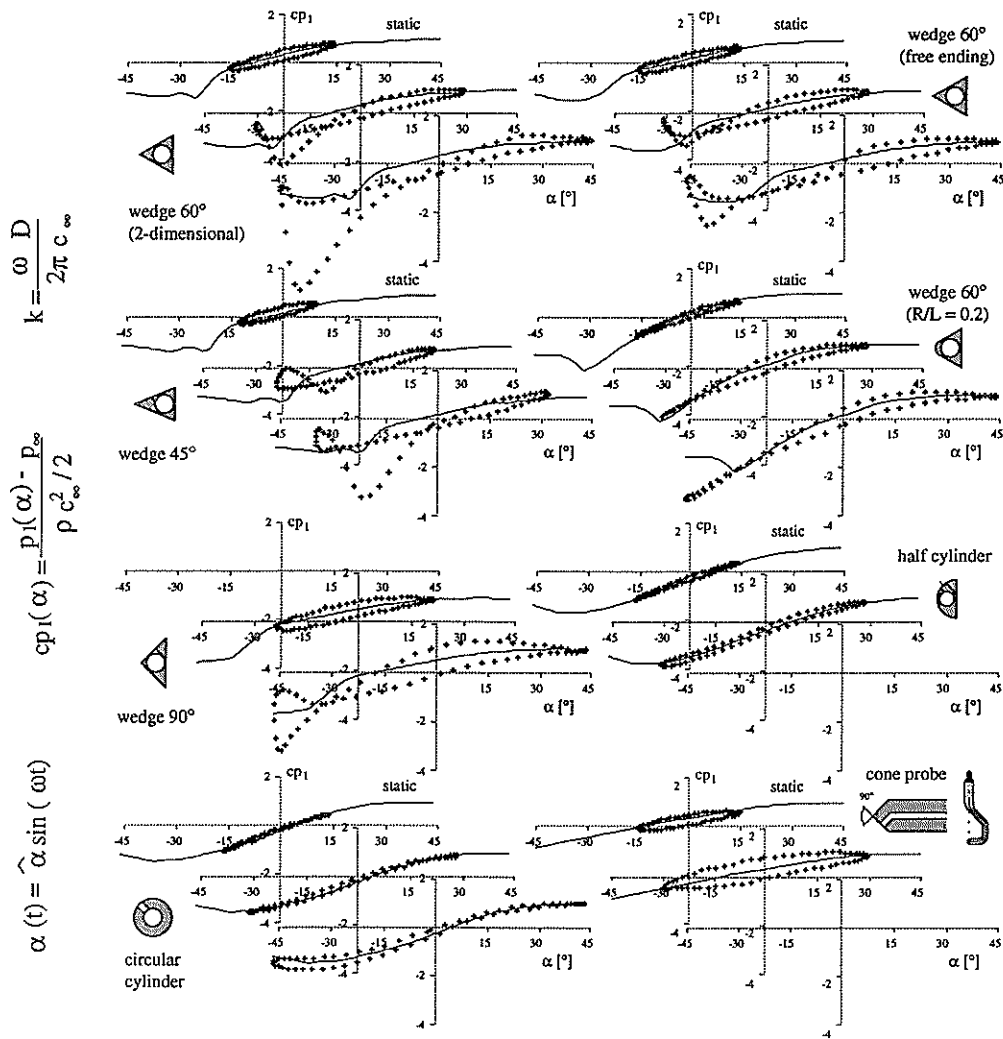

Figure 3.1-1 Dynamic calibration data as a function of the yaw angle α for different probes (k = 0.1, $15° < \hat{\alpha} < 45°$)

The different probes show wide spread properties. Measurement errors that may arise in some cases, if static calibration data are used alone to evaluate signals containing dynamic components, were discussed in HUMM/VERDEGAAL (1992A). The predominant dynamic effects identified were due to circulation, inertia, moving-wall, dynamic stall and synchronized vortex shedding. The analysis of the experimental results showed that the majority of measurement

errors due to these effects are directly proportional to the probe size. This is expressed by the relations for the reduced frequency k ~ D (D = probe diameter). Additionally, the extent of the resulting errors is strongly dependent on the probe geometry.

When discussing the dynamic effects it is interesting what analogies can be found in the literature. E.g. in helicopter aerodynamics the predominant effect causing the lift of the rotors to increase so enormously is *dynamic stall*. After the bursting of a laminar separation bubble a separated vortex propagates rearwards from the leading edge causing a transient pressure drop on the surface. In figure 3.1-1 a similar pressure drop can be seen to take place for all wedges when the amplitude of oscillation $\hat{\alpha}$ is increased beyond the static stall angle α_s ($\alpha_s \approx 22°$, $30°$ and $45°$ for the $45°$-, $60°$- and $90°$-wedge, respectively). This transient, non deterministic dynamic effect was found to cause the most severe measurement errors.

In the case of turbulence measurement with fast-response probes the stochastic fluctuating pressures on the probe surface are measured. Due to the shedding of Kármán vortices these pressure signals are contaminated. In cases where the flow fluctuates periodically with a frequency close to the natural vortex shedding another kind of *vortex interaction* takes place. In the *synchronization* range the shedding of the Kármán vortices is completely driven by the external flow distortion (e.g. k ≈ 0.2 for circular cylinders). This imposes a systematic effect on the dynamic probe characteristics (HUMM/VERDEGAAL 1992A).

Regarding distortions due to Kármán vortices, they can be reduced when applying sharp trailing edges on the probes (e.g. wedges) or an afterbody (e.g. 3D cone). As it was found in GIZZI (1994) these interactions cannot be significantly reduced when using half instead of full cylinders, whereas the characteristics of the 3D-cone were found to be superior in comparison to all other geometries. However, the results in figure 3.1-1 show that for the latter systematic deviations between dynamic and static calibration data are quite high. This is undoubtedly due to the fact that the probe stem imposes a circulation on the flow field around the probe tip. Concerning systematic dynamic characteristics the ones of the half cylinder are similar to the circular cylinder (figure 3.1-1).

In experiments a correlation between errors due to circulatory effects and static aerodynamic characteristics was sought. For this purpose holographic interferograms were taken in air under pure static conditions. At a Mach number of 0.7 different probe bodies were inserted into the flow under different angles of attack. From the holographic fringe pattern the pressure distribution on the probes was determined. By numerical integration of the pressures the lift forces acting on the probes could be determined (shown in figure 3.1-2 for the example of $\alpha = 10°$, Ma = 0.7) and plotted as a function of the angle of attack (figure 3.1-3).
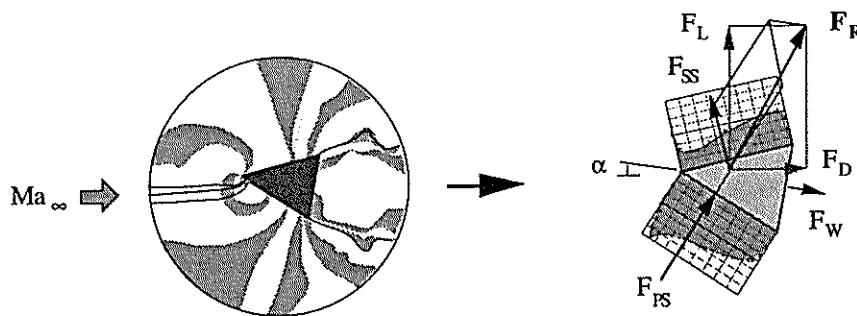

Figure 3.1-2 Hologram of the flow around a wedge and resulting static lift force F_L

The change of lift versus yaw angle $\partial c_L / \partial \alpha$ at $\alpha = 0°$ was then derived and qualitatively compared to the dynamic errors obtained in the model-experiments.
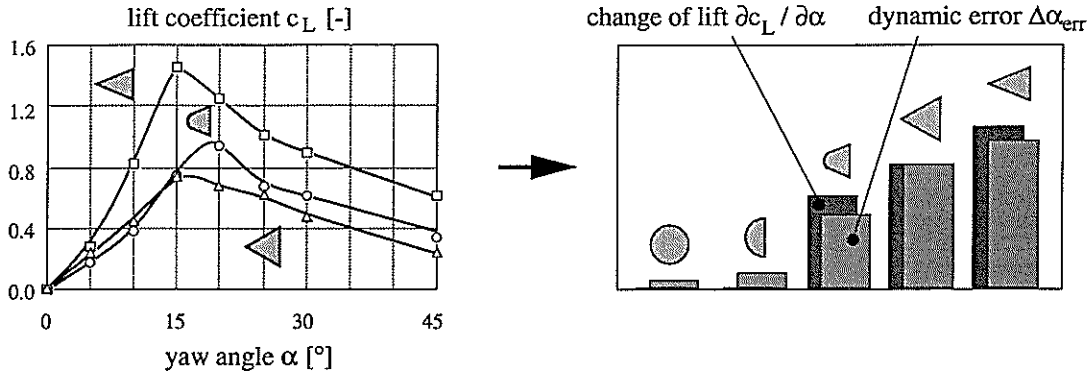

Figure 3.1-3 Correlation between dynamic errors and change of static lift $\partial c_L / \partial \alpha$

Although the two experiments were performed under completely different conditions the correlation is excellent. However, the results themselves are not surprising. It seems logical that probes changing their lift force drastically as a function of the flow angle exhibit a pronounced dynamic behaviour. On the other hand, circular and half cylinders, which produce no static lift, can be seen to be almost insensitive to dynamic effects.

This type of dynamic effect (circulation) exhibits a systematic behaviour. As long as no dynamic stall and synchronisation occur a linear correlation $\Delta\alpha_{err} \sim \partial c_L / \partial\alpha_{(\alpha = 0)}$ k α could be established. Under the same conditions inertia effects can be seen to show a systematic behaviour $\Delta\alpha_{err} \sim k^2 \hat{\alpha}$. Only when the Reyonolds numbers based on probe diameter are too high $(Re_D > 10^5)$ *moving-wall effects* gain in importance (HUMM/VERDEGAAL 1992A).

3.2 PITCH ANGLE OSCILLATIONS

Additional experiments comprised investigations of the influence of dynamic pitch angle fluctuations. Two types of circular cylinders and a 3D hemispherical probe were oscillated in the pitch angle plane. The probes were equipped with four (circular cylinder no. 1) or five sensing holes. In each case sensing hole 0 is used for total pressure measurement, 1 and 2 for yaw angle and 3 and 4 for pitch angle measurement (figure 3.2-1).
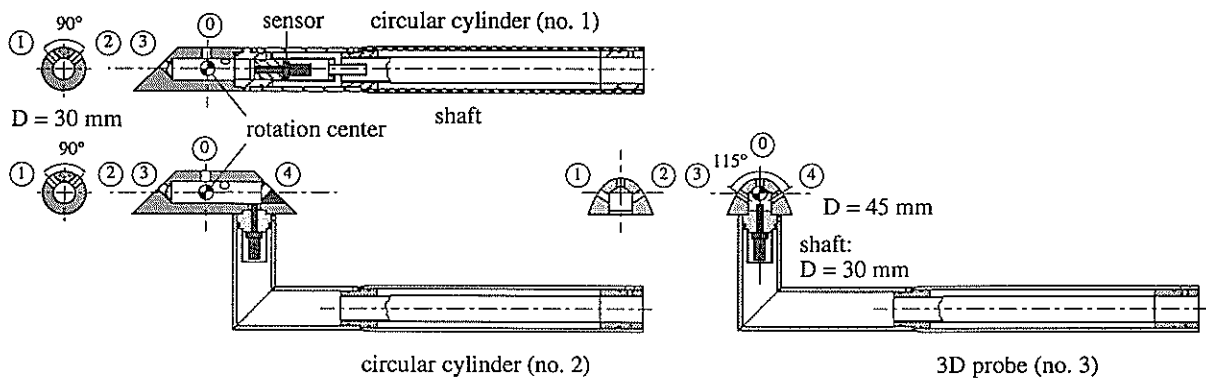

Figure 3.2-1 Probe geometries for pitch angle oscillations

The experimental set-up was arranged that the probe head was located in the center of the rotation. The probe shaft had a length of 300 mm and in order to avoid distortions from the sur-

face the probes were placed 250 mm beneath the water level. This led to high mechanical stresses when the oscillating probes were towed in the water. In order to keep drag and inertia forces low the experiments were confined to a Reynolds number of Re = 10'000 and reduced frequencies k < 0.20.

In figure 3.2-2 the non-dimensional pressures $cp_i = (p_i - p_\infty) / (\rho\, c_\infty^2 / 2)$ registered in the different sensing holes (0, 1 and 3) are plotted versus the pitch angle γ (t) of the experiment.
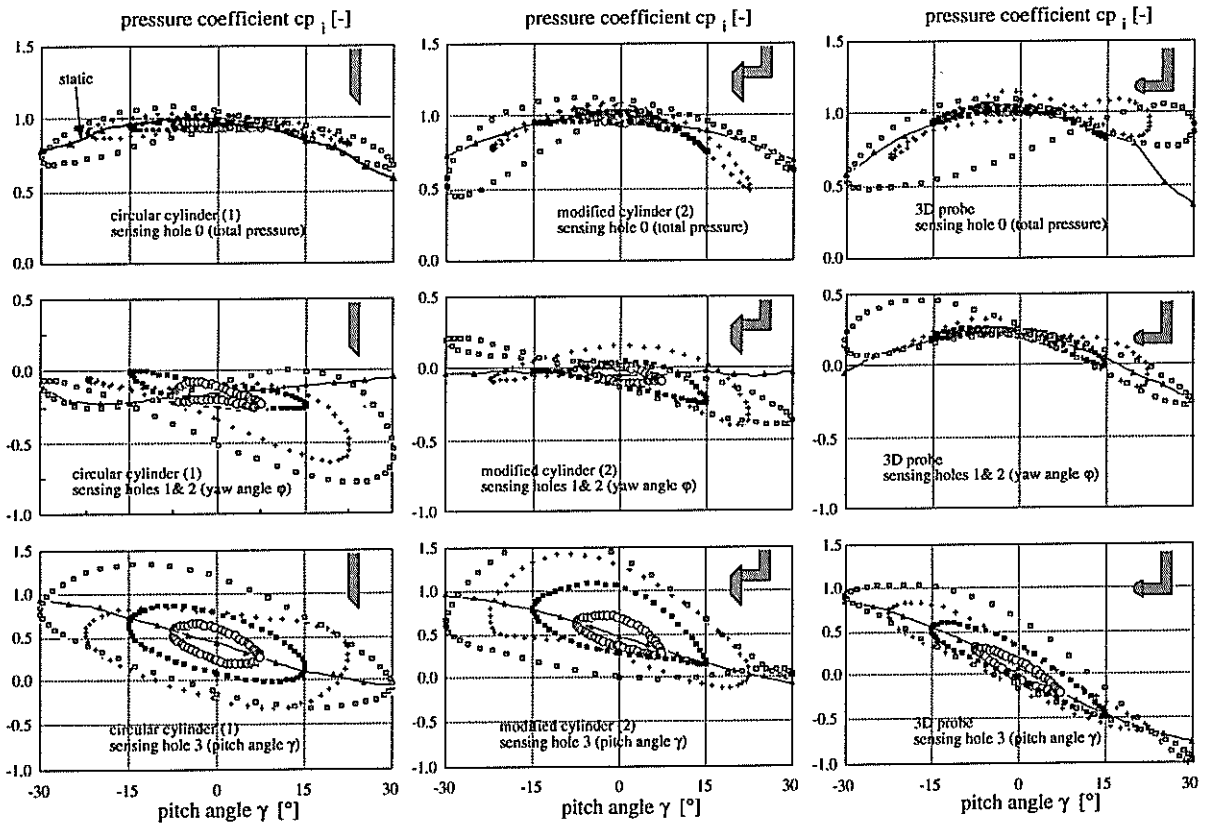

Figure 3.2-2 Dynamic and static calibration in the pitch angle plane; k = 0.1, $7.5 < \hat{\gamma} < 30°$

The results show that the dynamic effects have a strong influence on the pressure readings. Generally for low amplitudes of oscillation ($\hat{\gamma} < 15°$) the pressures registered in the sensing hole 0 for total pressure measurement is little affected by pitch angle oscillations. On the other hand, especially the pressure in sensing hole 3 for pitch angle measurement can be seen to be strongly affected. In this case the modified circular cylinder no. 2 shows the same characteristic as no. 1 whereas the hemi-spherical 3D probe is a factor of 2 less affected by dynamic effects. For the latter the probe stem has to be considered responsible for the occurrence of these effects since the probe head itself imposes no circulation on the flow field. These observings are in agreement with the ones in section 3.1 for a similar probe type.

No physical explanation could be found for the curve cp_3 (γ) with circular cylinder no. 1 ($\hat{\gamma}$ = 22.5°). It is most likely due to the fact that for this case the processing of the pressure signal was performed with respect to an unpropper trigger signal.

The influence of the oscillation parameters (frequency and amplitude) is illustrated in figure 3.2-3. For this purpose the procedures described in HUMM/VERDEGAAL (1992A) are applied. It

was shown that for yaw angle oscillations a circulatory term proportional to the first derivative of the angular motion $\gamma(t) = \hat{\gamma} \sin(\omega t)$ of the experiment occurs. Additionally a term due to inertia was seen to contribute a dynamic term proportional to the angular acceleration. When processing the data recorded under dynamic conditions using static calibration characteristics maximum error angles $\Delta\gamma_{err}$ in pitch angle measurement due to circulation and inertia can be quantified. Since circulation effects act proportionally to $d\gamma / dt$ they become maximum at $\omega t = 0°$ of the sinusoidal angular motion whereas for inertia acting proportionally to $d\gamma^2 / dt^2$ the influence is greatest at $\omega t = 90°$.
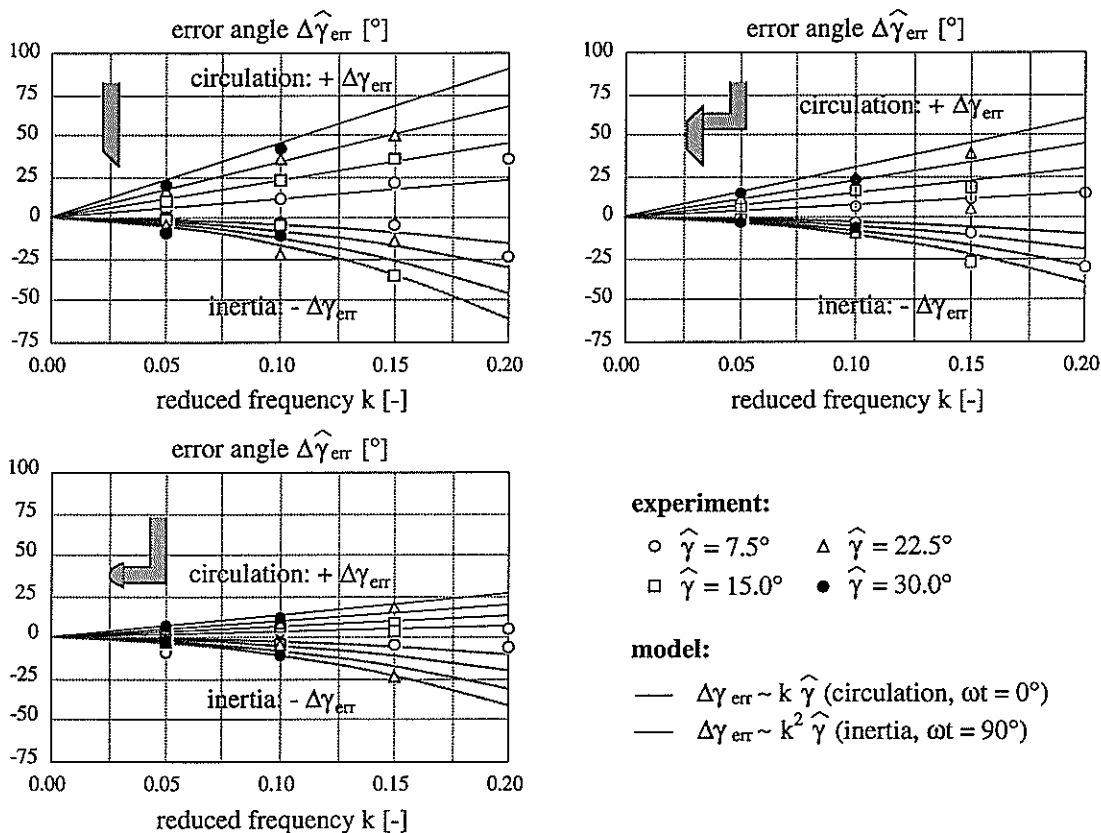

Figure 3.2-3 Maximum error angles $\Delta\gamma_{err}$ due to circulation ($\omega t = 0°$) and inertia ($\omega t = 90°$)

In the range $0 < k < 0.10$ the circulatory term dominates the dynamic response of the pressure in sensing hole 3 and such the error angles $\Delta\gamma_{err}$ due to circulation become greatest. In the figure a linear relation between reduced frequency k and amplitude of oscillation $\hat{\gamma}$ can be seen. Despite the scatter of the data inertia effects can be seen to occur proportional to $\hat{\gamma} k^2$. These findings, which are in excellent agreement with the ones for yaw angle oscillations in HUMM/VERDEGAAL (1992A), are important when discussing the suitability of probes for measurements in turbomachines (see section 3.4).

3.3 LONGITUDINAL OSCILLATIONS

To investigate the influence of velocity fluctuations on the pressure reading of aerodynamic probes the oscillating mechanism was modified according to figure 2-1 (C). In the experiments the mechanism performed sinusoidal oscillations in the longitudinal direction. Superposing this motion and the constant towing velocity c_0 within the water the probes were subjected to a flow with a time dependent velocity

$$c_\infty(t) = c_0\left(1 + \frac{\hat{c}}{c_0}\cos{(\omega t)}\right)$$ (3-3)

In figure 3.3-1 the pressures p (t) - p_∞ measured at four positions on a 60°-wedge probe for different yaw angles α are plotted versus the velocity c_∞ (t).

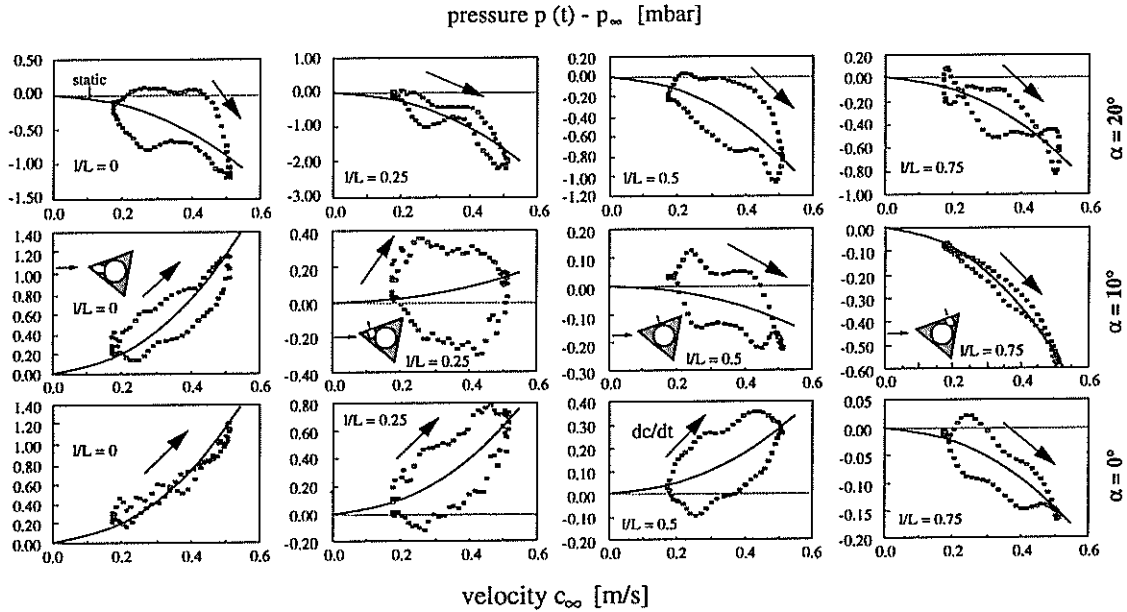pressure p (t) - p_∞ [mbar]

velocity c_∞ [m/s]

Figure 3.3-1   Indicated pressures p (t) - p_∞ at four relative positions (0 < l/L < 0.75, L denoting the side length) of a wedge probe as a function of c_∞ (t)
k = 0.1 and $\hat{c}$ / c_0 = 0.5 (arrows denote increasing velocity)

The discrepancies between the dynamic and static characteristics in figure 3.3-1 show that the effects are enormous. In comparison to the true value proportional to ρ c_∞^2 / 2 in most cases the indicated pressure is higher when the velocity is increasing. This is in agreement with the findings in KOVASZNAY et al. (1981) where it is postulated that the probe registers a quasi static value and a term proportional to the acceleration of the flow.

The influence of the relative flow angle α and position of the sensing hole can best be illustrated in figure 3.3-2. For each configuration as shown in figure 3.3-1 the constant B in equation 3-4 according to the relations after KOVASZNAY et al. (1981)

$$p\,(t) - p_\infty = cp_{static}\,\frac{\rho\,c^2\,(t)}{2} + B\,\rho\,\frac{D}{2}\frac{dc}{dt}\,(t)$$ (3-4)

was determined using a least squares approximation to model the measured values p (t) - p_∞. cp$_{static}$ represents a static calibration coefficient and B can be termed "inertia-coefficient". The same procedure was applied to the results of a circular cylinder and a wedge probe with a Pitot-type extension. This type of wedge probes is usually used for total pressure measurements in turbomachines.
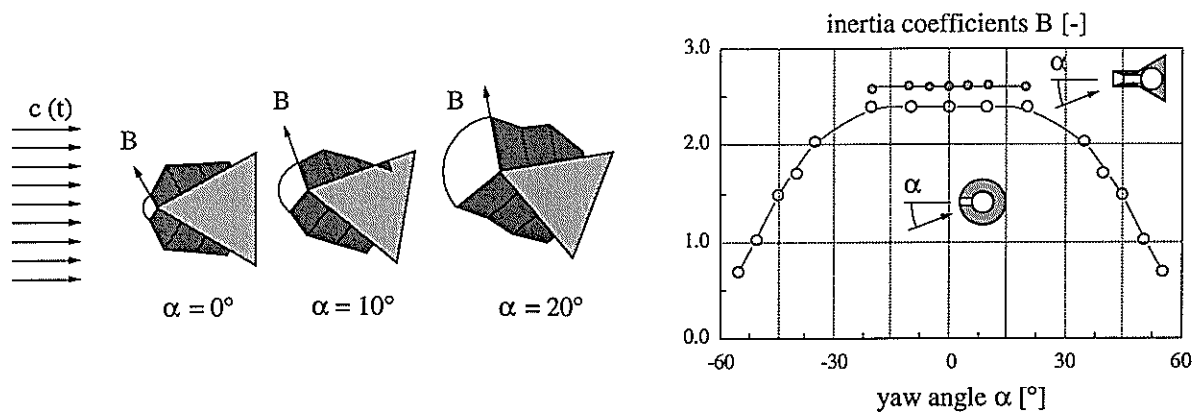
Figure 3.3-2   Added mass coefficients B for wedge probes and a circular cylinder

For the sharp nosed wedge the added mass coefficients vary remarkably for the different sensing holes and as well a pronounced influence of the yaw angle can be seen. Note that B at the leading edge varies by almost a factor of 4 when yawing the probe from $\alpha = 0$ to 20°. This will make a compensation of the dynamic effects, as described in chapter 4, very difficult.

Considering the curves p (t) - p_∞ in figure 3.3-1 it can be seen that other effects are prominent which are not taken into account by eq. 3-4. Apart from measurement uncertainties aerodynamic effects such as transient circulatory effects for $\alpha \neq 0$ (see e.g. FÖRSCHING 1974), dynamic stall, vortex interaction etc. may be responsible for the "non-linearity" of the results.

In comparison to the sharp-nosed wedge the results of the wedge with a Pitot-type extension and especially the circular cylinder show a far more systematic behaviour according to eq. 3-4. Additionally it is advantageous that the coefficients B do not change their magnitude within a range of approximately -20 < α < 20°.

In order to illustrate the universality of relations after equation 3-4 the values B obtained for various oscillation parameters are shown in figure 3.3-3.
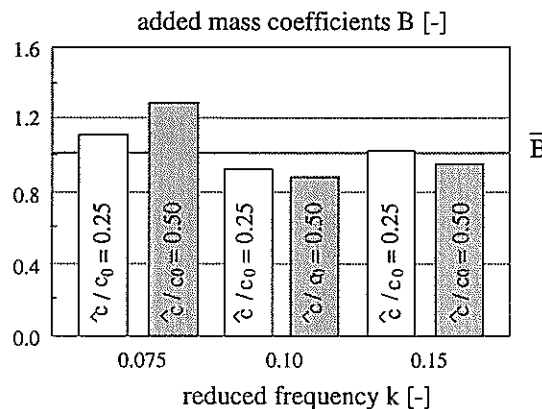

Figure 3.3-3   Added mass coefficients B for the wedge probe ($\alpha = 0$, relative position of the sensing hole l/L = 0.5)

The closer examination of the relations given in HUMM/VERDEGAAL (1992A) reveals that the effects due to inertia are nearly proportional to the reduced frequency k and relative amplitude of the oscillation $\hat{c}$ / c_0. Since k ~ D again the size of the probe can be seen to responsible for the magnitude of measurement errors.

3.4 DISCUSSION

In some cases measurement errors due to dynamic effects can be largely avoided using an appropriately shaped probe. For inevitable effects a systematic correlation may be established. This enables the user to model dynamic effects and correct measurement errors (chapter 4).

The suitability of aerodynamic probes for a measurement task has to be decided in context with given flow conditions inside the turbomachine. In HUMM et al. (1994) measurement errors due to dynamic and static aerodynamic effects for probes with different geometries and sizes were investigated. For this purpose the exit flow of a radial compressor wheel was considered where a sinusoidally fluctuating flow with a frequency of approximately 6 kHz was simulated. The AC part of the time dependent velocity due to systematic and random (turbulence) fluctuations was estimated to amount to $\pm$ 20% of the free stream velocity. A typical range of yaw angle fluctuations (sum of a systematic and random part) was determined to be $\hat{\alpha} \approx \pm 25°$. These parameters are in close agreement with the fast-response probe measurements reported in GYARMATHY et al. (1991). In many turbomachinery applications fluctuations in the meridional plane (pitch angle) are much less pronounced. E.g. from 3D measurements (HENEKA 1983A&B and SHREEVE/NEUHOFF 1984) one may conclude that $\hat{\gamma} \approx \pm 5°$ is a typical value.

The investigations in HUMM et al. (1994) revealed the remarkable fact that for prismatic circular cylinders errors due to yaw angle fluctuations are practically negligible. Also cylindrical probes exhibit far superior static aerodynamic characteristics in comparison to e.g. wedge probes.

Regarding pitch angle fluctuations the response of prismatic circular cylinders can be seen to be greater affected in comparison to a 3D-cone probe (section 3.2). However, since the amplitudes of pitch angle fluctuations typically are small these disadvantages are far outweighed by the superior behaviour when exposed to yaw angle fluctuations (see section 3.1).

According to the investigations presented in section 3.3 for circular cylinders and wedge probes with Pitot-type extension, inertia effects due to longitudinal velocity fluctuations are of the same magnitude. The effects can be minimized by reducing the probe size, while remaining measurement errors can be corrected during the data processing. The same is true for remaining circulatory and inertia effects due to pitch angle fluctuations.
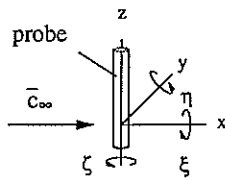
4. MODELLING AND COMPENSATION OF DYNAMIC EFFECTS

The discussion of the experimental results in chapter 3 has shown the importance of the probe geometry. In some cases dynamic effects deteriorating the quality of the measurement can be almost completely avoided when choosing the appropriate probe design. On the other hand, some other effects remain and deteriorate the quality of the measurement. As long as these effects are systematic (and deterministic) they can be taken into account. For this purpose in mathematical models the relations between pressures indicated by probes and flow fluctuation have to be established. To do so the overall forces and moments acting on the probe body due to dynamic flow conditions have to be considered.

The procedures serve as the basis for the compensation of dynamic effects during the data processing. The aim of the compensation is to apply corrections to the string of experimental data such that the true time history is reconstructed.

Modelling of Dynamic Effects

In 3D flows the dynamic response of the pressure p_j indicated in sensing hole j of the probe is a function of the overall forces and moments acting on the probe body due to velocities and accelerations. It is such necessary to employ two 6 by 6 matrices to model the forces and moments in a universal manner (eqs. 4-1 and 4-2).

$$
\begin{bmatrix} F_x \\ F_y \\ F_z \\ M_\xi \\ M_\eta \\ M_\zeta \end{bmatrix}
=
\begin{bmatrix}
A_{xx} & A_{xy} & A_{xz} & A_{x\xi} & A_{x\eta} & A_{x\zeta} \\
A_{yx} & A_{yy} & A_{yz} & A_{y\xi} & A_{y\eta} & A_{y\zeta} \\
A_{zx} & A_{zy} & A_{zz} & A_{z\xi} & A_{z\eta} & A_{z\zeta} \\
A_{\xi x} & A_{\xi y} & A_{\xi z} & A_{\xi\xi} & A_{\xi\eta} & A_{\xi\zeta} \\
A_{\eta x} & A_{\eta y} & A_{\eta z} & A_{\eta\xi} & A_{\eta\eta} & A_{\eta\zeta} \\
A_{\zeta x} & A_{\zeta y} & A_{\zeta z} & A_{\zeta\xi} & A_{\zeta\eta} & A_{\zeta\zeta}
\end{bmatrix}
\begin{bmatrix} c_x \\ c_y \\ c_z \\ \xi \\ \eta \\ \zeta \end{bmatrix}_{\text{velocity}}
\tag{4-1}
$$

$$
p_j = f\left(\sum F_i + \sum M_i\right) + \left(\sum F_{\dot i} + \sum M_{\dot i}\right)
$$

$$
\begin{bmatrix} F_{\dot x} \\ F_{\dot y} \\ F_{\dot z} \\ M_\xi \\ M_\eta \\ M_\zeta \end{bmatrix}
=
\begin{bmatrix}
B_{xx} & B_{xy} & B_{xz} & B_{x\xi} & B_{x\eta} & B_{x\zeta} \\
B_{yx} & B_{yy} & B_{yz} & B_{y\xi} & B_{y\eta} & B_{y\zeta} \\
B_{zx} & B_{zy} & B_{zz} & B_{z\xi} & B_{z\eta} & B_{z\zeta} \\
B_{\xi x} & B_{\xi y} & B_{\xi z} & B_{\xi\xi} & B_{\xi\eta} & B_{\xi\zeta} \\
B_{\eta x} & B_{\eta y} & B_{\eta z} & B_{\eta\xi} & B_{\eta\eta} & B_{\eta\zeta} \\
B_{\zeta x} & B_{\zeta y} & B_{\zeta z} & B_{\zeta\xi} & B_{\zeta\eta} & B_{\zeta\zeta}
\end{bmatrix}
\begin{bmatrix} \dot c_x \\ \dot c_y \\ \dot c_z \\ \ddot\xi \\ \ddot\eta \\ \ddot\zeta \end{bmatrix}_{\text{acceleration}}
\tag{4-2}
$$

With the aid of equation 4-1 the static calibration and circulation effects are modelled and 4-2 represents the "added-mass matrix" modelling forces and moments due to inertia (see e.g. BLEVINS 1979). Phenomena such as dynamic stall effects can not be modelled, since they are not deterministic. Further synchronisation effects have to be considered as the limitation of the procedures described in this chapter (see section 3.1). This implies that no wedges must be used and that the probe size has to be small enough, that $k = f\, D / c_\infty \ll 0.2$.

The discussion of the equations is much easier, when the coordinates are transformed from Cartesian into spherical. The matrices then become much simpler, but the coefficients are now a function of the flow angles α and γ (yaw and pitch).

$$
\text{velocity:} \quad
\begin{bmatrix} F_c \\ M_{\dot\alpha} \\ M_{\dot\gamma} \end{bmatrix}
=
\begin{bmatrix}
A_{cc} & A_{c\alpha} & A_{c\gamma} \\
A_{\alpha c} & A_{\alpha\alpha} & A_{\alpha\gamma} \\
A_{\gamma c} & A_{\gamma\alpha} & A_{\gamma\gamma}
\end{bmatrix}
(\alpha, \gamma)
\begin{bmatrix} c \\ \dot\alpha \\ \dot\gamma \end{bmatrix}
\tag{4-3}
$$

$$
\text{acceleration:} \quad
\begin{bmatrix} F_{\dot c} \\ M_{\ddot\alpha} \\ M_{\ddot\gamma} \end{bmatrix}
=
\begin{bmatrix}
B_{cc} & B_{c\alpha} & B_{c\gamma} \\
B_{\alpha c} & B_{\alpha\alpha} & B_{\alpha\gamma} \\
B_{\gamma c} & B_{\gamma\alpha} & B_{\gamma\gamma}
\end{bmatrix}
(\alpha, \gamma)
\begin{bmatrix} \dot c \\ \ddot\alpha \\ \ddot\gamma \end{bmatrix}
\tag{4-4}
$$

As for equation 4-3 the three coefficients A_{ic} to the left are obtained from the static calibration of the probe whereas the coefficients $A_{i\alpha}$ and $A_{i\gamma}$ have to be determined in experiments under dynamic conditions. The coefficients $A_{i\alpha}$ and $A_{i\gamma}$ represent the circulation effects due to angular velocities. All the coefficients B_{ij} in the "added-mass matrix", modelling inertia effects, have to be determined in a dynamic flow environment. Note that for non-nulled probes the coefficients B_{ic} contain as well a transient circulatory term (see chapter 3.3). Since $B_{ic} = f\,(\alpha, \gamma)$ it can be derived that in this case a velocity fluctuation imposes a moment M_α and M_γ.

The equations 4-1 through 4-4 must comply with the relations usually applied in aerodynamics. The coefficients B_{ic} represent added masses per unit length $m^* \sim B \rho D^2$ [kg/m] and $B_{i\alpha}$, $B_{i\gamma}$ an added mass moment $J^* \sim B \rho D^4$ [kg m^2/ m].

E.g. for static flow conditions the probe faces a drag force $F_D = c_D \rho c_\infty^2 / 2 D$ per unit length. This implies that $A_c = A_{cc} + A_{\alpha c} + A_{\gamma c} = f (\alpha, \gamma) = c_D (\alpha, \gamma) D \rho c_\infty / 2$. Analogous the moment per unit length due to the angular velocity $\dot\alpha$ must become $M_\alpha \sim C \rho c_\infty D^3 \dot\alpha$ (e.g. FÖRSCHING 1974). C represents a geometry-dependent constant, which may be termed $\partial c_L /$ $\partial\alpha$ (see figure 3.1-3). Such e.g. $A_{\alpha\alpha} \sim \partial c_L / \partial\alpha \rho c_\infty D^3$ and when determining a non-dimensional moment c_M acting on the probe, eq. 4-5 can be written

$$c_M = \frac{M_\alpha}{\rho c_\infty^2 / 2 D^2} \sim \frac{\partial c_L}{\partial\alpha} \frac{D \dot\alpha}{c_\infty} \qquad (4\text{-}5)$$

For sinusoidal oscillations $\alpha (t) = \hat\alpha \sin (\omega t)$ the maximum value for $D \dot\alpha / c_\infty$ can be replaced by the non-dimensional expression $2 \pi k \hat\alpha$. The moment c_M then becomes $\sim \partial c_L / \partial\alpha k \hat\alpha$. This is in excellent agreement with the experimental results in HUMM/VERDEGAAL (1992A) and the ones in figure 3.2-3 for pitch angle fluctuations, where measurement errors due to circulation are proportional to $k \hat\gamma$.

Compensation of Dynamic Effects

The compensation procedure is described for the example of 2D oscillatory flow using a circular cylinder for flow measurement. According to eqs. 4-3 and 4-4 the pressure indicated in a sensing hole of the probe is the sum of a quasi static and a dynamic term which can be written in a simplified form as shown in eq. 4-6.

$$p (t) = \overline{P_\infty} + \boxed{cp (\alpha) \frac{\rho c^2(t)}{2}} + \boxed{C_{\dot c} (\alpha) \frac{dc (t)}{dt}} + \boxed{C_{\dot\alpha} (\alpha) \frac{d\alpha (t)}{dt} + C_{\ddot\alpha} (\alpha) \frac{d^2\alpha (t)}{dt^2}} \qquad (4\text{-}6)$$

(quasi static) (dynamic: longitudinal) (angular oscillation)

$\overline{P_\infty}$ is assumed to be constant, cp represents a static calibration coefficient and the constants C_i are obtained from the dynamic probe calibration. If e.g. a circular cylinder is used, where dynamic effects due to angular oscillations (yaw angle α) can practically be neglected, the total pressure indicated by the forward facing sensing hole becomes

$$p_0 (t) = \overline{P_\infty} + cp (\alpha) \frac{\rho c^2 (t)}{2} + C_{\dot c} (\alpha) \frac{dc}{dt} \qquad (4\text{-}7)$$

To derive the velocity c from the measured data $p_0 (t)$ a non-linear differential equation would have to be solved. If the AC part of $c (t) = c_0 + c' (t)$ is small the relation can be linearized and $c^2 (t) = (c_0 + c' (t))^2 \approx c_0^2 + 2 c_0 c' (t)$. In this case equation 4-7 can be solved with the aid of the numerical approach proposed by STEARNS (1975). The true pressure $p_{rec, m}$ in point m is then "reconstructed" from two measured samples p_{m-1} and p_m.

$$p_{rec, m} = \frac{1}{T} [(T - 1 + e^{-T}) p_m - (T e^{-T} - 1 + e^{-T}) p_{m-1}] + e^{-T} p_{rec, m-1} \qquad (4\text{-}8)$$

In equation 4-8 the non-dimensional constant T is proportional to the time between two sampling points and has to be determined empirically from a reference case.

How well this works is demonstrated in figure 4-1. In the experiment a circular cylinder for total pressure measurement was exposed to a flow with a fluctuating velocity. The known true stagnation pressure $\rho\, c_\infty^2$ (t) / 2 was then reconstructed from the indicated values p (ωt) - p_∞.
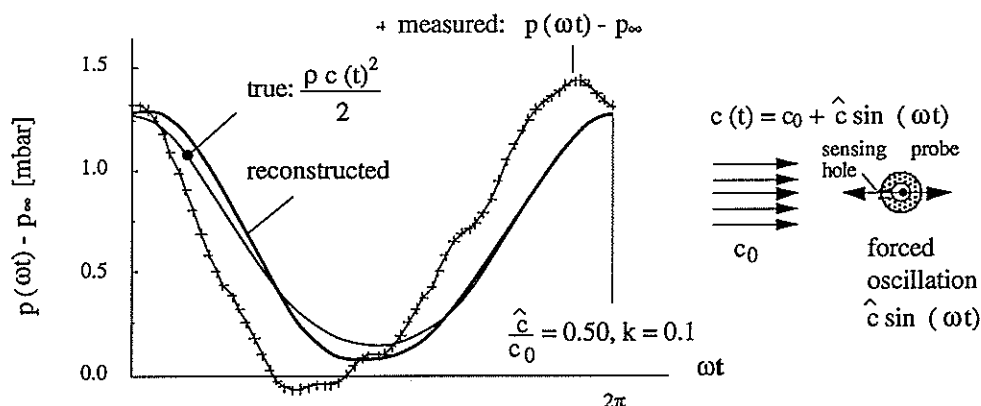

Figure 4-1 Reconstruction of the true stagnation pressure $\rho\, c^2$ (t) / 2 over one period of oscillation $(0 < \omega t < 2\pi)$

Between reconstructed and true stagnation pressure only minor discrepancies can be seen. This is most likely due to measurement uncertainties and the fact that the procedure according to eq. 4-8 is only valid for linear differential equations.

5. CONCLUSIONS

One of the main objectives of the aerodynamic probe design should be to eliminate errors due to dynamic effects. An important step in this direction is the choice of an appropriate probe shape.

Prismatic circular cylinders can be seen to be largely free of errors with respect to yaw angle fluctuations. On the other hand, their dynamic response is affected by velocity and pitch angle fluctuations. Whereas the influence of the latter is in most cases negligible, inertia effects due to velocity fluctuations are inevitable since probes have a finite size (this limitation is due to manufacture, sensor technology as shown in KUPFERSCHMIED et al. 1994). However, the analysis of these effects shows that, within a practical range, they are systematic. Such a modelling and hence a correction of inertia effects using compensation procedures becomes feasible. Note that similar procedures can be applied to correct the measurement signals falsified by static aerodynamic effects like e.g. velocity gradients, which show a systematic behaviour (HUMM/VERDEGAAL 1992B).

6. ACKNOWLEDGEMENTS

7. LIST OF SYMBOLS

c velocity [m/s]

D probe diameter [mm], [m]

f frequency of oscillation [Hz]

k reduced frequency [-]; $k = f D / c_\infty$

$\widehat{(..)}$ amplitude of oscillation

α yaw angle [°], [rad]; in the model-experiments $\alpha (t) = \widehat{\alpha} \sin (\omega t) = \widehat{\alpha} \sin (2\pi f t)$

$\dot{\alpha}$ angular velocity [s^{-1}]; for sinusoidal oscillation $\dot{\alpha} (t) = \omega \widehat{\alpha} \cos (\omega t)$

$\ddot{\alpha}$ angular acceleration [s^{-2}]; for sinusoidal oscillation $\ddot{\alpha} (t) = - \omega^2 \widehat{\alpha} \sin (\omega t)$

8. REFERENCES

BLEVINS D.R. 1979: "Formulas for Natural Frequency and Mode Shape; Chapter 14: Structural Vibrations in a Fluid"; *Robert E. Krieger Publishing Company*

FÖRSCHING H.W. 1974: "Aeroelasticity"; *Springer (in German)*

GIZZI W.P. 1994: "Investigations of Dynamic Effects on Probe Measurements"; *Diploma Thesis, Swiss Federal Institute of Technology Zurich* (in German)

GOSSWEILER C., HERTER D., KUPFERSCHMIED P., 1992: "Fast-Response Probe Measurements in a Turbulent Pipe Flow"; *Proceedings of the 11th Symposium on Measuring Techniques for Transonic and Supersonic Flows in Cascades and Turbomachines, Munich, Germany*

GYARMATHY G., HUNZIKER R., RIBI B., SPIRIG M. 1991: "On the Change of Impeller Non-Uniformities with Flow Rate in a Centrifugal Compressor"; *IMechE, C423/053*

HENEKA A. 1983A: "Development and Application of a Wedge Probe for Unsteady 3D Flow Measurement in Turbomachines"; *PhD-Thesis, University Stuttgart, Germany (in German)*

HENEKA A. 1983B: "Unsteady 3D Flow Measurement in Turbomachines Using Wedge Probes"; *VDI-Report Nr. 487 (in German)*

HUMM H.J., GOSSWEILER C., GYARMATHY G. 1994: "On Fast-Response Probes, Part 2: Aerodynamic Design Studies"; *ASME GT Conference The Hague, Netherlands 94-GT-27*

HUMM H.J., VERDEGAAL J.I. 1992A: "Aerodynamic Design Criteria for Fast-Response Probes"; *Proceedings of the 11th Symposium on Measuring Techniques for Transonic and Supersonic Flows in Cascades and Turbomachines, Munich, Germany*

HUMM H.J., VERDEGAAL J.I. 1992B: "Investigation of the Influence of Velocity Gradients on Measurements with a Wedge Probe", *Technical Note 92-06, Swiss Federal Institute of Technology, Turbomachinery Laboratory (in German)*

KOVASZNAY L.S.G., TANI I., KAWAMURA M., FUJITA H. 1981: "Instantaneous Pressure Distribution Around a Sphere in Unsteady Flow"; *Journal of Fluids Engineering Vol. 103*

KUPFERSCHMIED P., GOSSWEILER C.R.. GYARMATHY G. 1994: "Aerodynamic Fast-Response Probe Measurement Systems: State of Development, Limitations and Future Trends"; *Proceedings of the 12th Symposium on Measuring Techniques for Transonic and Supersonic Flows in Cascades and Turbomachines, Prague, Czech Republic*

McCROSKEY W.J. 1977: "Some Current Research in Unsteady Fluid Dynamics-THE 1976 FREEMAN SCOLAR LECTURE"; *Journal of Fluids Engineering, Vol. 99, March 1977*

NAUDASCHER E. 1991: "Hydrodynamic Forces"; *University of Karlsruhe, A.A. Balkema, Rotterdam, Brookfield*

SHREEVE R.P., NEUHOFF F. 1984: "Measurements of the Flow From a High-Speed Compressor Rotor Using a Dual Probe Digital Sampling (DPDS) Technique"; *Journal for Engineering for Gas Turbines and Power, Vol. 106*

STEARNS, S.D. 1975: "Digital Signal Analysis"; *Hayden Book Company N.Y., U.S.A.*